Open Access Library Journal
2024, Volume 11, e9526
ISSN Online: 2333-9721
ISSN Print: 2333-9705

Influence of Sludge Concentration and Hydraulic Load on the Puratory Performance of Drying Beds with Unsaturated Flow

Téténa Martial Yéo[1,2], Kinanpara Koné[1,2,3*], Yao Francis Kouamé[1], Kotchi Yves Bony[1,3], Théophile Gnagne[4]

[1]Department of Environment, University Jean Lorougnon Guédé, Daloa, Côte d'Ivoire
[2]Laboratory of Environmental Sciences and Technologies, Department of Environment, University Jean Lorougnon Guédé, Daloa, Côte d'Ivoire
[3]Laboratory of Biodiversity and Tropical Ecology, Department of Environment, University Jean Lorougnon Guédé, Daloa, Côte d'Ivoire
[4]Laboratory of Geosciences and Environment, Department of Sciences and Environmental Management, University Nangui Abrogoua, Abidjan, Côte d'Ivoire
Email: *kkinanpara@gmail.com

How to cite this paper: Yéo, T.M., Koné, K., Kouamé, Y.F., Bony, K.Y. and Gnagne, T. (2024) Influence of Sludge Concentration and Hydraulic Load on the Puratory Performance of Drying Beds with Unsaturated Flow. *Open Access Library Journal*, **11**: e9526.
https://doi.org/10.4236/oalib.1109526

Received: November 4, 2022
Accepted: November 9, 2024
Published: November 12, 2024

Abstract

Unsaturated Flow Drying Beds effectively treat septic sludge from septic tanks. However, the sustainability of this purification process depends on the organic load applied and the availability of oxygen. To guarantee this sustainability, a flow model in an unsaturated medium coupled with the variation of the biofilm was developed. The calibration, validation, and comparison of experimental and simulation results were carried out on the basis of the NASH criterion. The experimental results show that for the organic load of 34 $mgO_2/cm^2/d$, when the sludge with a concentration of 2537 mgO_2/l is applied to the hydraulic load 4.28 cm/d, the purification efficiency is 95%. On the other hand, for the same organic load, when the sludge with a concentration of 1175 mgO_2/l is applied to the hydraulic load of 10 cm/d, the purification efficiency is 79%. The simulation results confirm this paradox of purification yields. They reveal that for a sludge with a concentration of 2537 mgO_2/l applied to a hydraulic load of 4.28 cm/d, most of the pollution is retained in the first four centimeters of the filter beds with a residence time of 6h26mn. On the other hand, for a sludge with a concentration of 1175 mgO_2/l applied to a hydraulic load of 10 cm/d, the pollution goes down to a depth of 13 cm with a residence time of 4h21mn. Therefore, unsaturated flow drying bed technology makes it possible to easily treat heavily loaded fecal sludge at low hydraulic loads. Which thus guarantees good purifying efficiency and slows down clogging.

Subject Areas

Hydrology

Keywords

Concentration, Sludge, Hydraulic Load, Purification Performance

1. Introduction

The Unsaturated Flow Drying Bed (UFDB) is an essentially aerobic purification process that is part of the purification processes by cultures fixed on supports. As a result, the organic load (Co) applied and the availability of oxygen are essential factors for its operation [1] [2] [3]. The applied organic load (Co) is the amount of pollution applied per day and per unit area. It is the product of hydraulic head (Ch) and sludge concentration (So).

Several authors have shown the purifying capacity of UFDB. Indeed, [4] and [5] have shown that sand with a medium particle size is the best filter bed with the need for lateral aeration. [6] revealed more significant efficiencies in the elimination of microbiological and physicochemical parameters from sludge. COD and NTK are eliminated by more than 95% and a reduction of 4 Ulog of feacal coliforms. A strategy for eliminating nitrogen from sludge was determined by [1]. However, everyone was confronted with the problem of the sustainability of UFDB.

The results of experimental tests from the treatment of septic tank sludge by UFDB show that for the same organic load (Co), the purification yields are better for high concentrations of sludge (So) than for low concentrations of sludge (So).

The objective of this study is to explain this paradox highlighted by these experimental results to guarantee the durability and purification performance of the UFDB technology, through digital simulation in two stages:

- The establishment of the paradox by the simulation of the inequality of purification yields for an organic load (Co) fixed with two types of faecal sludge of different concentrations (So) and hydraulic loads (Ch) depending on whether $So1 > So2$ and that $Ch1 < Ch2$.
- The highlighting of the combination of explanatory factors which are: 1) The microbial biofilm, 2) the free porosity to the flows and 3) the residence times.

2. Material

The material is composed of the experimental device and the faecal sludge. The experimental device consists of two cylindrical plastic columns with a capacity of 220 liters and an internal diameter of 54 cm each (**Figure 1**). They contain sand. Above each column, there is a diffuser which ensures a good distribution of the effluent on the infiltration surface. The faecal sludge used comes from different septic tanks.

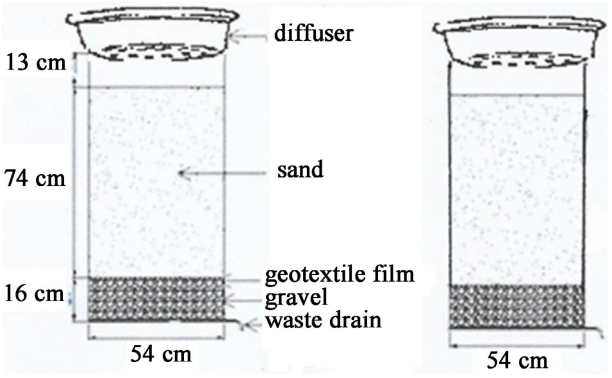

Figure 1. Diagram of the experimental device.

3. Methods

3.1. Experimental Measurements

The device works by an instantaneous supply of a fixed organic load by alternating one day of feeding and two days of rest. At each addition of sludge, the flow rates at the outlet of each column are measured until the flow stops.

The water content of the massifs (θ) is measured by weighing the sample before and after drying. The difference in mass between these two states of the sample corresponds to the mass of water it contained. This mass divided by the mass of the sample corresponds to the value of the specific humidity.

The hydrogen potential (pH), the chemical oxygen demand (COD) and nitrogen (NTK) concentrations of raw and treated faecal sludge are determined using the physicochemical analysis methods summarized in Table 1.

Table 1. Summary of analytical methods.

Parameters	Methods
COD (mgO_2/L)	Oxidability to potassium dichromate (AFNOR T 90-101)
NTK	Spectrophotometry after mineralization (AFNOR T 90-110)
pH	Electrometry using a HACH EC 10 type field pH meter

3.2. Modeling of Hydrodynamic and Hydrokinetic Functioning

Formulation of water transfer mechanisms

In wastewater treatment using UFDB technology, the flow takes place in an unsaturated porous medium. Water transfers are therefore described by DARCY's law generalized to flows in unsaturated porous media (Equation (1)) and by the continuity law (Equation (2)) [7] [8]:

$$q(\theta) = -K(\theta)\frac{\partial H}{\partial z} \quad (1)$$

With $q(\theta)$ = DARCY velocity (cm/s); θ = humidity by volume (m^3/m^3) which is between the residual humidity (θ_r) and the humidity at saturation (θ_s); $H = h - z$ = total load (cm); h = load representative of soil water pressure (cm) which is a

function of soil moisture; z = dimension counted positively downwards (cm); $K(\theta)$ hydraulic conductivity (cm/s) which is a function of humidity or head representative of soil water pressure (h). Assuming that water is incompressible, the continuity equation is written.

$$\frac{\partial\theta}{\partial t} = -\frac{\partial q(\theta)}{\partial z} \tag{2}$$

By combining the DARCY equation (Equation (1)) and the continuity equation (Equation (2)), we obtained the equation of motion (Richards equation):

$$\frac{\partial\theta}{\partial t} = \frac{\partial}{\partial z}\left[K(\theta)\frac{\partial h(\theta)}{\partial z} - K(\theta)\right] \tag{3}$$

If we designate by $C(h(\theta)) = \frac{\partial\theta}{\partial h(\theta)}$ the phenomena of capillarity and by $D(\theta) = \frac{K(\theta)}{C(h)}$ the hydraulic diffusivity, then the equation Equation (3) has become:

$$\frac{\partial\theta}{\partial t} = \frac{\partial}{\partial z}\left[D(\theta)\frac{\partial\theta}{\partial z} - K(\theta)\right] \tag{4}$$

It is accepted that the flow within a sandy massif is essentially gravitational and that the hydraulic diffusivity is low and constant also showed that the flow within a sand mass can be assimilated to a piston flow. Capillarity phenomena are therefore negligible. Under these conditions, the equation Equation (4) has become:

$$\frac{\partial\theta}{\partial t} = -\frac{\partial}{\partial z}\left[K(\theta)\right] \tag{5}$$

The resolution of this differential equation requires the knowledge of the analytical relation which links the hydraulic conductivity to the water content ($K(\theta)$). As part of this model, the formula of Van Genuchten (2005) is used [9]:

$$K(\theta) = K_s\left(\frac{\theta-\theta_r}{\theta_s-\theta_r}\right)^{\frac{1}{2}}\left[1-\left(1-\left(\frac{\theta-\theta_r}{\theta_s-\theta_r}\right)^{\frac{1}{m}}\right)^{m}\right]^2 \tag{6}$$

With θ_s = saturation humidity of the porous medium (m^3/m^3); θ_r = residual humidity of the porous medium (m^3/m^3); m = parameter linked to the air-ground contact surface.

Formulation of the variation of the fixed biomass

The variation in microbial biomass under the double effect of assimilation and endogenous respiration is written as follows:

$$\frac{\partial\rho_{bio}}{\partial t} = \gamma * R_{DCO} - K_d\left(\frac{C_{oxy}}{K_{oxy}+C_{oxy}}\right)\rho_{bio} \tag{7}$$

The first term (R_{DCO}) of the second member represents the consumption (assimilation) of the substrate equivalent to the bacterial growth while the second term expresses the endogenous respiration equivalent to the bacterial decay.

Bacterial growth is predominant during the assimilation phase, when there is an abundance of oxygen and substrate. On the other hand, during the endogenous respiration phase, when there is an abundance of oxygen and a lack of substrate, bacterial growth predominates [10].

$$R_{DCO} = \frac{\mu_m}{\gamma}\left[\frac{C_{DCO}}{K_{DCO}+C_{DCO}}\right]\left[\frac{C_{oxy}}{K_{oxy}+C_{oxy}}\right]\rho_{bio} \tag{8}$$

ρ_{bio} = biomass content (mg/cm); γ = yield of conversion of the substrate into biomass; K_d = biomass self-regulation coefficient; K_{oxy} = half-activity concentration of oxygen in the biofilm; C_{DCO} = DCO concentration (mg/cm); μ_m = maximum growth rate of microorganisms; K_{DCO} = DCO half-activity; C_{oxy} = concentration of oxygen in the gas phase (mg/cm).

By replacing in Equation (7), R_{DCO} by its expression (Equation (8)), we obtained the following equation:

$$\frac{\partial\theta_{bio}}{\partial t} = \left[\mu_m\left(\frac{C_{DCO}}{K_{DCO}+C_{DCO}}\right) - K_d\right]\left[\frac{C_{oxy}}{K_{oxy}+C_{oxy}}\right]\theta_{bio} \tag{9}$$

With $\rho_{bio} = \frac{\theta_{bio}}{\lambda}$: humidity relative to the biofilm.

The resolution of this equation implies the knowledge of the relation which describes the variation of COD and that which describes the variation of oxygen within the purifying mass. The variation of the COD in the porous medium can be described through the equation Equation (10), [10] [11]:

$$\begin{aligned}\frac{\partial(\theta C_{DCO})}{\partial t} &= \frac{\partial}{\partial z}\left(\theta D_{DCO}(\theta)\frac{\partial C_{DCO}}{\partial z} - qC_{DCO}\right)\\ &\quad -\frac{\mu_m}{Y}\left(\frac{C_{DCO}}{K_{DCO}+C_{DCO}}\right)\left(\frac{C_{oxy}}{K_{oxy}+C_{oxy}}\right)\rho_{bio}\end{aligned} \tag{10}$$

Similarly, the variation of oxygen in the gaseous phase of the purification mass can be described by the following equation:

$$\begin{aligned}&\frac{\partial(\theta_s-\theta)C_{oxy}}{\partial t} = \frac{\partial}{\partial z}\left((\theta_s-\theta)D_{oxy}(\theta)\frac{\partial C_{oxy}}{\partial z}\right)\\ &-\left(\gamma\mu_m\left(\frac{C_{DCO}}{K_{DCO}+C_{DCO}}\right)\left(\frac{C_{oxy}}{K_{oxy}+C_{oxy}}\right)+\alpha K_d\left(\frac{C_{oxy}}{K_{oxy}+C_{oxy}}\right)\right)\rho_{bio}\end{aligned} \tag{11}$$

The formulation of the different purification mechanisms resulted in a system of four nonlinear partial differential equations which are: The water transfer equation, the COD transfer equation, the oxygen transfer equation and the microbial variation equation. The state variables of the system thus obtained are: The water content, the COD concentration, the oxygen concentration and the microbial biomass content.

3.3. Discretization of Partial Differential Equations

For each of the equations which constitute the system to be solved, the method of

resolution by finite differences is adopted. The values of the state variables are determined at each internal node of the filter bed.

Hydrodynamic equation

The discrete form of the equation which estimates the value of the flows at each internal node of the purification mass is as follows:

$$q = -K(\theta)\frac{h(\theta)_{i+1}^{j} - h(\theta)_{i}^{j}}{\Delta z} + K(\theta) \tag{12}$$

However, it is assumed that the suction phenomena are negligible. This hypothesis led to an equality between q and $K(\theta)$. Under these conditions, the discretization of the hydrodynamic equation (Equation (12)) led to the following form:

$$\theta_i^{j+1} = \theta_i^j + \frac{\Delta t}{\Delta z}\left[K\left(\theta_{i+1}^j\right) - K\left(\theta_i^j\right)\right] \tag{13}$$

In this relation, i and j are the indices of the spatio-temporal components z and t.

Oxygen transfer equation

The discretization of the equation with partial derivatives of the transfers of oxygen made it possible to obtain the expression Equation (14).

$$\begin{aligned} {C_{oxyi}}^{j+1} = {} & \frac{\theta_s - \theta_i^j - w_i^j}{\theta_s - \theta_i^{j+1} - w_i^{j+1}}{C_{oxyi}}^{j} + \frac{\theta_s - \theta_i^j - w_i^j}{\theta_s - \theta_i^{j+1} - w_i^{j+1}}\frac{D_{oxy}\left(\theta_i^j, w_i^j\right)\Delta t}{\Delta z^2}\left({C_{oxyi}}^{j} - 2{C_{oxyi}}^{j} + {C_{oxyi}}^{j}\right) \\ & - \left|\frac{\mu_m}{\gamma}\left(\frac{{C_{DCOi}}^{j}}{K_{DCO} + {C_{DCOi}}^{j}}\right)\left(\frac{{C_{oxyi}}^{j}}{K_{oxy} + {C_{oxyi}}^{j}}\right) + \alpha K_d\left(\frac{{C_{oxyi}}^{j}}{K_{oxy} + {C_{oxyi}}^{j}}\right)\right|\frac{\Delta t}{\theta_s - \theta_i^{j+1} - w_i^{j+1}}\rho_i^j \end{aligned} \tag{14}$$

COD transfer equation

The discretization of the COD transfer equation led to the expression below.

$$\begin{aligned} {C_{DCOi}}^{j+1} = {} & \frac{\theta_i^j}{\theta_i^{j+1}}{C_{DCOi}}^{j} + \frac{\theta_i^j}{\theta_i^{j+1}}\frac{\Delta t}{\Delta z^2}D_{DCO}\left(\theta_i^j\right) * \left({C_{DCOi+1}}^{j} - 2{C_{DCOi}}^{j} + {C_{DCOi-1}}^{j}\right) \\ & - \frac{\Delta t}{\theta_i^{j+1}\Delta z}\left(K\left(\theta_{i-1}^j\right) * {C_{DCOi+1}}^{j} - K\left(\theta_i^j\right) * {C_{DCOi}}^{j}\right) \\ & - \frac{\Delta t\,\mu_m}{\theta_i^{j+1} Y}\left(\frac{{C_{DCOi}}^{j}}{K_{DCO} + {C_{DCOi}}^{j}}\right)\left(\frac{{C_{oxyi}}^{j}}{K_{oxy} + {C_{oxyi}}^{j}}\right)\rho_{bio} \end{aligned} \tag{15}$$

Equation of the variation of the microbial biofilm

The amount of biofilm at each internal node of the filter bed is calculated from the following relationship:

$$\rho_i^{j+1} = \rho_i^j + \left|\mu_m\left(\frac{{C_{DCOi}}^{j}}{K_{DCO} + {C_{DCOi}}^{j}}\right)\left(\frac{{C_{oxyi}}^{j}}{K_{oxy} + {C_{oxyi}}^{j}}\right) - K_d\right|\Delta t \tag{16}$$

3.4. Algorithm

The software used as support is the IPOX software, designed from the HYDRUS Version 5.0 software. The different programs of its 11 source files are written in

FORTRAN 77. Compilation and development are done under FORTRAN PowerStation Version 4.0/Microsoft Developer Studio.

Verification of the fit of the model is made by analyzing the NASH coefficient (NTD) defined by equation Equation (17. The values of the coefficients can only be retained if the NASH coefficient (NTD) is greater than or equal to 70% (Deschesne *et al.*, 2005; Hangen *et al.*, 2005).

$$\mathrm{NTD} = 1 - \frac{\sqrt{\sum_{i=1}^{n}\left(d_{ci} - d''_{ci}\right)^2}}{\sum_{i=1}^{n}\left(d_{oi} - d''_{oi}\right)^2} \tag{17}$$

d_{ci} = calculated; d_{oi} = observed data; d''_{ci} = mean of the calculated data; d''_{oi} = mean of obersved data.

3. Results

3.1. Highlighting the Paradox of the Inequality of Purification Yields

To compare the results from the simulation with the experimental results, a simulation of DCO removal efficiencies is made on coarse sand whose hydrodynamic characteristics are presented in Table 2.

Table 2. Hydrodynamic characteristics of coarse sand.

Sand Parameters	θ_s	θ_r	K_s (cm/s)	n	α
Values	0.62	0.03	0.0185	1.91	0.03

Based on the experimental results, the simulations are made at two organic loads (34 $mgO_2/cm^2/j$ and 45.36 $mgO_2/cm^2/j$ with j = d = day) for five months under the conditions presented in Table 3.

Table 3. Conditions for simulating faecal sludge treatment on coarse sand.

Organic loads, C_o (mg $O_2/cm^2/j$)	Case of figures	DCO Concentrations, S_o (mg O_2/l)	Hydraulic loads C_h (cm/j)
34	1st Case	1175	10
	2nd Cas	2537	4.28
45.36	1st Case	1175	12.5
	2nd Cas	2537	5.71

The results show that there is a good correlation between the simulated DCO values and those obtained experimentally. Indeed, the average value of the NASH coefficient is 0.85 (Figure 2).

Moreover, the results confirm that for the organic load of 34 $mgO_2/cm^2/j$, the yields are better when sludge with a concentration of 2537 mgO_2/l is applied to the hydraulic load of 4.28 cm/j; Compared to the case where sludge with a con-

centration of 1175 mgO_2/l is applied at a hydraulic head of 10 cm/j.

The same is true for the organic load 45.36 $mgO_2/cm^2/j$. When sludge with a concentration of 2537 mgO_2/l is applied at a hydraulic head of 5.71 cm/j, the yields are better than those obtained with sludge with a concentration of 1175 mgO_2/l, applied at a hydraulic head of 12.5 cm/j.

These results, therefore, show that it is with the most concentrated sludge that the best purification yields are obtained.

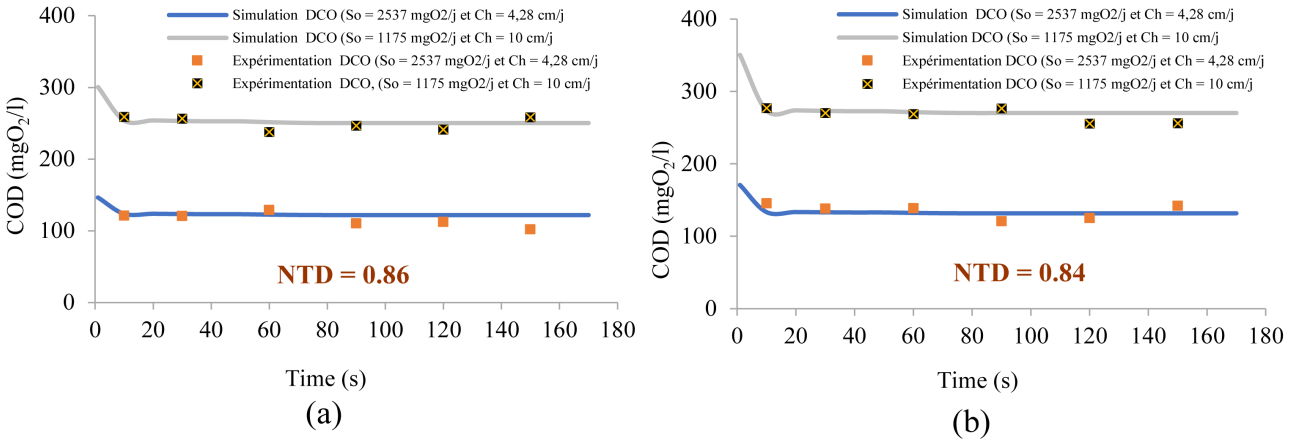

Figure 2. COD of filtrates for the same organic load but at different concentrations and at different hydraulic loads ((a) C_o = 34 $mgO_2/cm^2/j$, (b) C_o = 45.36 $mgO_2/cm^2/j$).

3.2. Highlighting the Combination of Explanatory Factors for the Difference in Yields

For all the simulations (simulation of the variation of the microbial biofilm, simulation of the variation of the free porosity to the flows and simulation of the variation of the residence times), the filter bed is made up of coarse sand (Table 2).

Besides, the simulation conditions are defined in Table 3 for the two organic fillers used.

3.2.1. Variation of Microbial Biofilm

The results of the simulation of the variation of the biofilm over two operating cycles show that for each organic load, the biofilm increases during the periods of feeding and decreases during the periods of rest (Figure 3).

The results also show that for a given organic load, biofilm growth during feeding periods is more intense for the highly concentrated substrate and applied at low hydraulic head compared to the low concentrated substrate applied at a high hydraulic head (Figure 3).

The maximum values of the microbial biomass obtained at the end of each feeding period are presented in Table 4.

The results also show that the resorption of the biofilm during rest periods is faster when the highly concentrated faecal sludge is applied at low hydraulic loads compared to the cases where the weakly concentrated sludge is applied at high hydraulic loads (Figure 3).

Table 4. Biofilm rate within beds at the end of two feeding periods for the same organic load but at different hydraulic loads and concentrations.

	34 mg $O_2/cm^2/j$		45.36 mg $O_2/cm^2/j$	
DCO Concentrations S_0 (mg O_2/l)	1175	2537	1175	2537
Hydraulic loads C_h (cm/j)	10	4.28	12.5	5.71j
Biofilm rate at the 1st feeding period (g/l)	0. 282	0.345	0. 300	0.382
Biofilm rate at the 2nd feeding period (g/l)	0. 335	0.446	0. 348	0.471

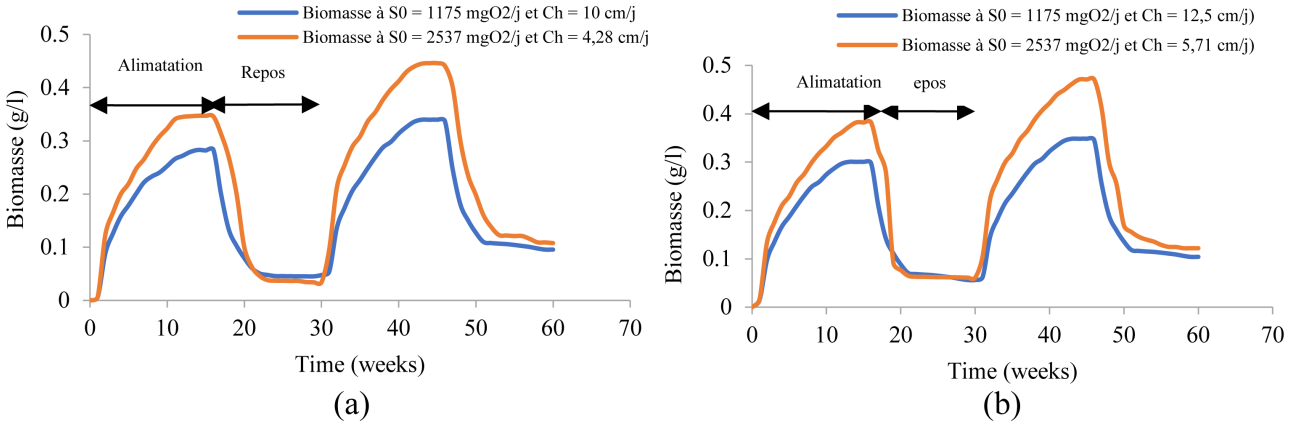

Figure 3. Microbial biomass rate during two operating cycles for the same organic load but at different concentrations and at different hydraulic loads ((a) C_o = 34 $mgO_2/cm^2/j$, (b) C_o = 45.36 $mgO_2/cm^2/j$).

3.2.2. Variation of the Free Porosity with Flows

The results of the simulation of the variation in humidity relative to the biofilm of filter beds show that, for the organic load of 34 $mgO_2/cm^2/j$, the maximum humidity value is 0.26 and is obtained at 13 cm depth for the couple (S_0 = 1175 mgO_2/l and C_h = 10 cm/j). On the other hand, for the pair (S_0 = 2537 mgO_2/l and C_h = 4.28 cm/j), it is equal to 0.35 and is obtained at a depth of 4 cm (**Figure 4(a)**).

For the organic load 45.36 $mgO_2/cm^2/j$, the maximum value of the humidity relative to the biofilm is 0.38 and is obtained at a depth of 16 cm for the couple (S_0 = 1175 mgO_2/l and C_h = 12.5 cm/j). With the couple (S_0 = 2537 mgO_2/l and C_h = 5.71 cm/j), the maximum humidity value is equal to 0.49 and is obtained at a depth of 7 cm (**Figure 4(b)**).

The different values of the free porosity to the flows which result from the variation of the humidity relative to the biofilm of the filtering masses are presented in **Table 5**. These results show that the reduction of the free porosity to the flows is greater when the sludge from draining, highly concentrated, are applied at low hydraulic heads compared to the case where, weakly concentrated, the sludge is applied at high hydraulic heads.

3.2.3. Variation of Residence Times

The variation in residence times is simulated from the variation in restitution flow rates which are simulated at organic loads of 34 $mgO_2/cm^2/j$ and 45.36 $mgO_2/cm^2/j$ under the same conditions as the variation in purification yields. The

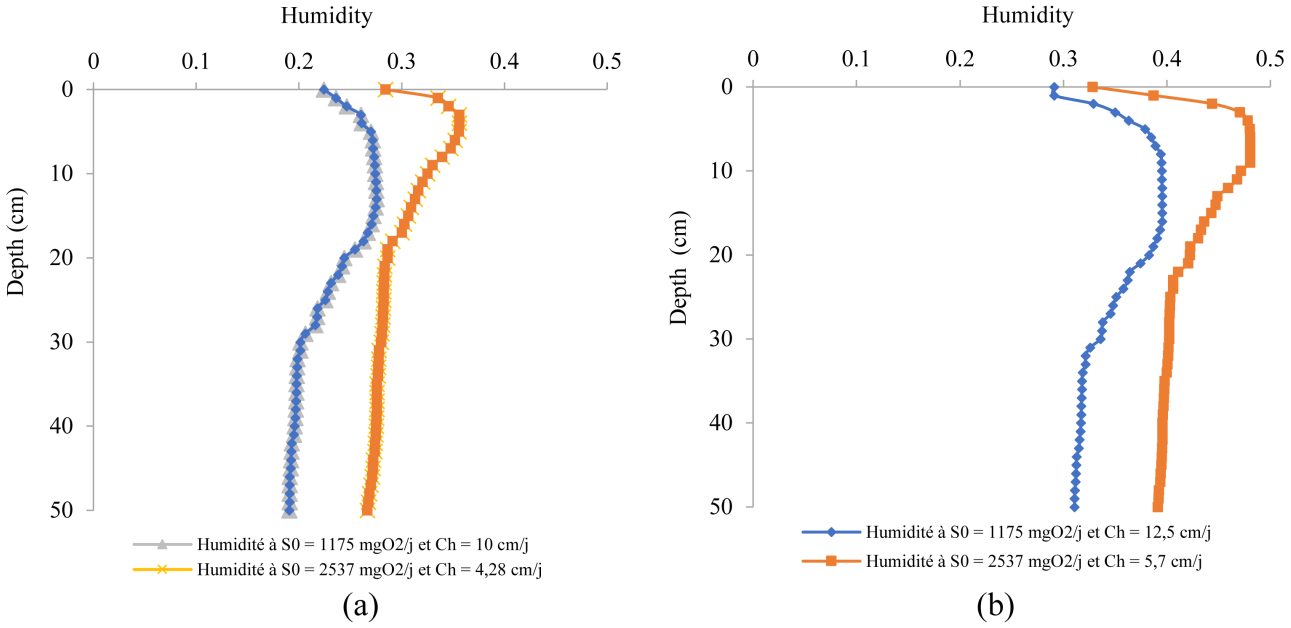

Figure 4. Humidity for the same organic flow but at different concentrations and at different hydraulic heads, ((a) C_o = 34 $mgO_2/cm^2/j$, (b) C_o = 45.36 $mgO_2/cm^2/j$)

Table 5. Free flow porosity for the same organic load but at different hydraulic loads and concentrations.

Organic loads (mg $O_2/cm^2/j$)	34		45.36	
DCO concentrations (mg O_2/l)	1175	2537	1175	2537
Hhydraulic loads (cm/j)	10	4.28	12.5	5.71
Free flow porosities	0.35	0.26	0.23	0.14
Depth of oxidation (cm)	13	4	16	7

results show that for each organic load, the restitution of the flows is faster when the hydraulic load is high. On the other hand, when the hydraulic head is low, the restitution is prolonged in time (Figure 5).

Thus, for the organic load 34 $mgO_2/cm^2/j$, when the hydraulic load is 10 cm/j, with a sludge of concentration equal to 1175 mgO_2/l, the maximum release rate is 159 cm^3/s. On the other hand, when the hydraulic head is 4.28 cm/j, with a sludge concentration equal to 2537 mgO_2/l, the maximum release rate is 108 cm^3/s (Figure 5(a)).

As for the organic load 45.36 $mgO_2/cm^2/j$, when the hydraulic load is 12.5 cm/j, with a sludge of concentration equal to 1175 mgO_2/l, the maximum restitution rate is 162 cm^3/s. On the other hand, when the hydraulic head is 5.71 cm/j, with a sludge concentration equal to 2537 mgO_2/l, the maximum release rate is 110.6 cm^3/s (Figure 5(b)).

The residence times which result from this variation in the release rates are presented in Table 6. The results show that the residence times are longer in the cases where high concentration sludges are applied at low hydraulic heads

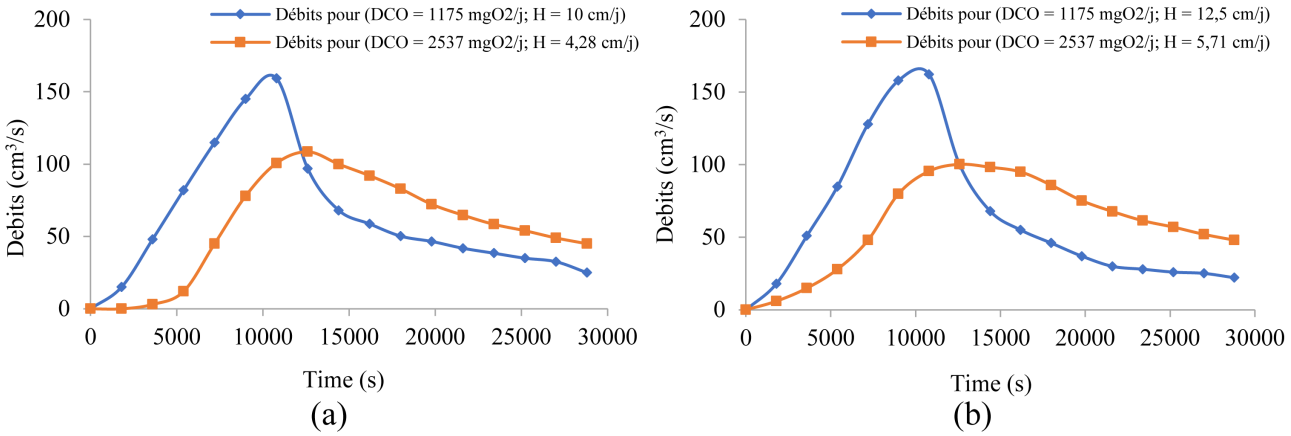

Figure 5. Restitution flow rates for the same organic flow applied at different concentrations and at different hydraulic heads ((a) C_o = 34 $mgO_2/cm^2/j$, (b) C_o = 45.36 $mgO_2/cm^2/j$).

Table 6. Residence time of sludge filtrates within coarse sand for the same organic load applied to hydraulic loads and different concentrations.

Organic loads (mg $O_2/cm^2/j$)	34		45.76	
DCO concentrations (mg O_2/l)	1175	2537	1175	2537
Hydraulic loads (cm/j)	10	4.28	12.5	5.71
Residence time	4 h 21 mn	6 h 26 mn	4 h 34 mn	6 h 40mn

compared to where low concentration slurries are applied at high hydraulic heads.

4. Discussion

The results show that the developed model reproduces well the real operation of the Unsaturated Flow Drying Bed (UFDB). Indeed, the comparison of the simulated results with the experimental results, provided a NASH coefficient estimated at 85% and which is greater than 70% [12] [13].

In terms of improving the understanding of the functioning of the UFDB, the model makes it possible to explain that it is easier to treat faecal sludge heavily loaded by the UFDB than faecal sludge with a low load; for a fixed organic load.

Indeed, the experimental results show that for the organic load of 34 $mgO_2/cm^2/j$, when sludge with a concentration of 2537 mgO_2/l is applied to the hydraulic load of 4.28 cm/j, the purification efficiency is 95%. On the other hand, for the same organic load of 34 $mgO_2/cm^2/j$, when sludge with a concentration of 1175 mgO_2/l is applied to the hydraulic load of 10 cm/j, the purification efficiency is 79%.

The results of the simulation not only confirm this paradox of purification yields, but also reveal that for a sludge with a concentration of 2537 mgO_2/l applied to a hydraulic head of 4.28 cm/j, most of the pollution is retained. in the first four centimeters of the filter beds and the residence time is 6h26mn. On the other hand, for a sludge with a concentration of 1175 mgO_2/l applied to a hydraulic head of 10 cm/j, the pollution descends to a depth of 13 cm and the residence time is

4h 21 mn.

The best purification yields obtained with high concentration sludges are linked to the low hydraulic loads to which these sludges are applied. Indeed, the results of the simulations show that for a low hydraulic head, the pollution is maintained near the infiltration surface where its oxidation is maximum due to the availability of oxygen. According to [14] and [3], highly concentrated sludge creates fairly large oxygen concentration gradients between the surface of the purification mass and the atmospheric air so that the diffusion of oxygen inside the filter bed is increased. In addition, the results of the simulations show that the residence time of the liquid fraction of the sludge within the porous medium is longer when highly concentrated slurries are applied at low hydraulic heads. Thus, the long pollution-biofilm contact time coupled with good oxygenation leads to good oxidation of nitrogen and carbon pollution.

Conversely, this is not the case for low-concentration sludge applied at a high hydraulic head. In this case, the simulation results show that the pollution goes deeper (13 cm), out of reach of the oxygen that diffuses from the infiltration surface. In addition, the high hydraulic heads reduce the residence time of the liquid fraction of the sludge within the filter beds. Under these conditions, according to [9] [15]-[18], the pollution does not have enough time to be well oxidized; hence the low purification yields.

Thus, from the perspective of a large-scale exploitation of the UFDB technology, it is easier to treat highly loaded faecal sludge by applying it to low hydraulic heads. In this case, good purification efficiency is guaranteed, the process of internal clogging of the massifs is slowed down and the reversibility of the clogging is accelerated when it occurs.

5. Conclusions

To simulate the hydrodynamic and biological mechanisms that ensure the elimination of pollution during the treatment of fecal sludge from septic tanks by UFDB; A model is designed. It has two modules representing hydrodynamic mechanisms and biological mechanisms. The adjustment of the model was made from the results of experiments carried out on two columns of sand.

The results reveal that it is easier to treat highly loaded faecal sludge by applying it at low hydraulic heads. This makes it possible to guarantee good purification efficiency, to slow down the process of internal clogging of the massifs and to accelerate the reversibility of the clogging when it occurs; Unlike the case where slurries with low organic loads are applied at high hydraulic loads.

Conflicts of Interest

The authors declare no conflicts of interest.

References

[1] Kouamé, Y.F., Yéo, T.M., Gnagne, T., Konan, K.F., N'gouandi, K.F., Yapo, O.B., Seka,

A. and Houenou, P.V. (2010) Strategy for Eliminating Nitrogen from Fecal Sludge Using Unsaturated Flow Drying Bed (UFDB). *Journal de la Société Ouest-Africaine de Chimie Note*, **29**, 1-10.

[2] Théophile, G., Martial, Y.T., Francis, K.Y. and Félix, K.K. (2014) Unsaturated Flow Drying Bed (UFDB): An Alternative for Treatment of Septic Tanks Sludge. *Journal of Water Resource and Protection*, **6**, 454-462. https://doi.org/10.4236/jwarp.2014.65045

[3] Yéo, T.M. (2018) Hydrodynamics, Hydrokinetics and Clogging of an Unsaturated Flow Drying Bed in the Treatment of Fecal Sludge from Septic Tanks. Unique Doctoral Thesis, Nangui Abrogoua University.

[4] Yéo, T.M., Koné, K., Gnagne, T. and Bony, K.Y. (2020) Influence of Granulometry on the Durability of the Non-Satured Flow Drying Bed in the Treatment of Septic Tank Sludge. *International Journal of Innovation and Applied Studies*, **29**, 275-286.

[5] Tenena Martial, Y., Kinanpara, K., Kotchi Yves, B., Yao Francis, K. and Theophile, G. (2021) Influence of the Side Ventilation on the Durability of the Functioning of Drying Beds With Non-Saturated Flow in Treatement of Septic Tank Sludge. *International Journal of Advanced Research*, **9**, 172-186. https://doi.org/10.21474/ijar01/12998

[6] Gnagne, T., Kouamé, Y.F. and Yéo, T.M. (2019) Design, Operation and Maintenance of Unsaturated Flow Drying Bed (UFDB) for Septic Tanks Sludge Treatment. *International Journal of Biological and Chemical Sciences*, **13**, 114-121.

[7] Peters, A. and Durner, W. (2009) Design and Performance of a Large Modular Zero-Tension Lysimeter for In-Situ Water Collection from Preferential Flow Paths European Geosciences Union (EGU) General Assembly.

[8] Koffi, K., Aubertin, M., Hernandez, M.A., Ouangrawa, M., Chapuis, R.P. and Bussiere, B. (2008) Study of the Hydraulic Conductivity of Mixtures with Spread Grain Sizes GeoEdmonton 2008. Edmonton: GeoEdmonton'08 Organizing Committee.

[9] Mubarak, I., Mailhol, J.C., Angulo-Jaramillo, R., Bouarfa, S. and Ruelle, P. (2009) Effect of Temporal Variability in Soil Hydraulic Properties on Simulated Water Transfer under High-Frequency Drip Irrigation. *Agricultural Water Management*, **96**, 1547-1559. https://doi.org/10.1016/j.agwat.2009.06.011

[10] Drouin, M. (2010) Modeling of Anisothermal Turbulent Flows in Macroporous Media Using a Double Filtering Approach. University of Toulouse.

[11] Bien, L.B. (2014) Transfers of Water and Solute in a Heterogeneous Unsaturated Medium on a Laboratory Pilot Scale. Doctoral Thesis, National Institute of Applied Sciences of Lyon, Doctoral School of Chemistry of Lyon.

[12] Dechesne, M., Barraud, S. and Bardin, J. (2005) Experimental Assessment of Stormwater Infiltration Basin Evolution. *Journal of Environmental Engineering*, **131**, 1090-1098. https://doi.org/10.1061/(asce)0733-9372(2005)131:7(1090)

[13] Hangen, E., Gerke, H.H., Schaaf, W. and Hüttl, R.F. (2005) Assessment of Preferential Flow Processes in a Forest-Reclaimed Lignitic Mine Soil by Multicell Sampling of Drainage Water and Three Tracers. *Journal of Hydrology*, **303**, 16-37. https://doi.org/10.1016/j.jhydrol.2004.07.009

[14] Wanko, A. (2005) Study of Transfer Mechanisms and Evaluation of the Oxygenation and Treatment Capacities of Devices by Cultures Fixed on Fine Granular Support. Doctoral Thesis No. 99026201, MSH Doctoral School, Mathematics and Information and Engineering Sciences.

[15] Racault, Y., Boutin, P. and Douat, J. (1984) Study by Tracing the Hydraulic Behavior

of a Purification Lagoon: Influence of the Geometry of the Basin. *French Journal of Water Sciences*, **3**, 107-218.

[16] Seguret, F. (1998) Study of the Hydrodynamics of Water Treatment Processes with Fixed Biomass, Application to Bacterial Beds and Biofilters. Mechanics Thesis, University of Bordeaux.

[17] Kaskassian, S., Gaudet, J.P., Chastanet, J., Decung, F., Angulo-Jaramillo, R., Szenknect, S., Côme, J.M., Getto, D., Barthes, V. and Krimissa, M. (2009) Projet ANR-PRECODD/ TRANSAT 2005-2009: Evaluation of Transfer times, in the Unsaturated Zone of Soils, of Dissolved Contaminants or Particles, Technical Guide.

[18] Kaskassian, S., Chastanet, J., Gleize, T., Come, J.M., Getto, D., Barthes, V. and Angulo-Jaramillo, R. (2012) The Infiltration Test Coupled with Non-Reactive Tracing: A Tool to Evaluate the Transfer of Pollutants in the Unsaturated Zone of the Soil, Water, Industry, Nuisances. *Water*, *Industry*, *Nuisances*, **349**, 38-45.